



Edited by:
Tünde Alapi
István Ilisz

Publisher:

University of Szeged, H-6720 Szeged, Dugonics tér 13,
Hungary

PROCEEDINGS OF THE
25th International Symposium
on Analytical and Environmental Problems

Szeged, Hungary
October 7-8, 2019



ISBN 978-963-306-702-4

2019.
Szeged, Hungary

University of Szeged

EVAPORATION OF LIQUIDS FROM POROUS FILMS – METHODOLOGY AND ANALYTICAL POSSIBILITIES

Ildikó Y. Tóth¹

¹Department of Applied and Environmental Chemistry, University of Szeged, Interdisciplinary Excellence Centre, H-6720, Szeged, Rerrich Béla tér 1, Hungary
e-mail: ildiko.toth@chem.u-szeged.hu

Abstract

The evaporation of liquids from porous films is a very complex phenomenon, which can be followed by simultaneous weight monitoring, electric resistance measurement and infrared imaging. The appropriate evaluation of these measurement results can carry both quantitative and qualitative analytical information. The aim of our recent work is to demonstrate this opportunity through the example of the evaporation of simple solvents from the porous buckypaper prepared from carbon nanotubes.

Introduction

Recent developments in nanotechnology have highlighted the importance of the classical topics of wetting, droplet spreading and evaporation due to their pronounced effect in technological applications (e.g., air/fuel premixing, micro-fluidics, oil recovery, etc.) [1,2]. Multiple phenomena take place simultaneously when a liquid droplet contacts a porous surface: wetting, spreading, capillary filling, gravity induced convective flow, adsorption, evaporation from the surface, evaporation from the pores, etc. The evaporation of a sessile droplet can be studied by several experimental methods: transmission electron microscopy, environmental scanning electron microscopy, contact angle measurement, high speed camera recordings, thermal imaging, just to name a few. The evaporation of sessile droplets can be followed by an equipment assembled at the Department of Applied and Environmental Chemistry, University of Szeged: this equipment can guide simultaneous weight monitoring, electric resistance measurement and infrared imaging at a controlled temperature (typically at 50 °C). There are several experimental results characteristic for the evaporation process, the most important ones being the total evaporation time, time of evaporation only from the surface, full width at half maximum of the time-dependent mass and resistance curves, evaporation rate, initial area of the droplet, and the wetted area at the moment of total evaporation from the surface, etc. [3-5].

The main goal of this work was to demonstrate the analytical possibilities of this method through the example of sessile droplet evaporation (water, 1-propanol, ethanol, heptane, acetonitrile) from porous buckypapers prepared from pristine non-functionalized carbon nanotubes (*nf*-CNT) and -COOH functionalized CNT (*f*-CNT).

Experimental

Materials: The multiwall carbon nanotubes were synthesized by 2 h of catalytic chemical vapor deposition from a C₂H₄:N₂ (30:300 cm³/min) gas mixture at 650 °C over Fe₂Co/Al₂O₃ catalyst (metal loading: 2.5-2.5 m/m%). The synthesized materials were purified by repeating 4 h of refluxing in 10 mol/dm³ aqueous NaOH, then 4 h in cc. HCl solution four times. Some pristine non-functionalized carbon nanotubes (*nf*-CNT) were subjected to oxidative chemical functionalization (8 h reflux of 4 g CNT in 500 cm³ cc. HNO₃ solution) to facilitate surface carboxyl group formation and improve their hydrophilicity to get so called functionalized carbon nanotubes (*f*-CNT). The typical length of CNTs was over 10 μm and their outer diameter fell in the 15-25 nm range as determined from TEM image analysis. CNTs were

converted into buckypaper (BP) by filtering 70 cm³ of their 0.1 g/dm³ suspensions through a 0.45 mm nominal pore diameter Whatmann nylon membrane filter. The *nf*-CNTs and *f*-CNTs were suspended by 40 min ultrasonication in N,N-dimethylformamide and water, respectively [3,4].

Methods: Liquid droplet evaporation (1-propanol, distilled water, ethanol, acetonitrile, heptane) was studied from both *nf*-CNT and *f*-CNT buckypaper films. The droplets (3-10 μL, 25 °C) were instilled with an Eppendorf Xplorer electronic pipette on the heated surface of the porous films (50 °C). The temperature, the electric resistance and weight variations were simultaneously monitored.

Buckypaper was placed onto a purpose-built sample holder and kept in place by a top piece that had a 0.7 cm diameter circular opening in it for placing the liquid droplet. The setup included a type K thermocouple in contact with the non-wetted part of the BP. The distance between the porous film and the heater was 1 cm. Data from the thermocouple was fed back to the temperature controller that maintained a base BP temperature of 50 ± 0.5 °C by continuously adjusting the heater power using fuzzy logic control.

The sample holder was placed on a Sartorius Cubis microbalance with 0.01 mg readability and the weigh variation during droplet evaporation was recorded.

For thermal imaging a FLIR A655sc infrared (IR) camera was used. This unit has a thermal sensitivity of 30 mK, an accuracy of ±2 °C for temperatures up to 650 °C at 640x480 resolution. Its uncooled microbolometer detector has a spectral range of 7.5-14.0 μm. The IR camera is equipped with a 2.9x (50 μm) IR close-up lens, with 32x24 mm field of view and 50 μm spatial resolution. The recorded images are transferred to a PC with FLIR ResearchIR Max software. Sessile droplet evaporation movies were acquired at maximum resolution with 50 Hz frame rate. Each CNT film's emissivity (ϵ_{film}) was determined by calibration at the initial film temperature (50 °C) with a black electrical tape ($\epsilon = 0.95$). During liquid surface evaporation the temperature was determined by taking into account the emissivity of the liquid ($\epsilon_L = 0.95$); after surface evaporation, the emissivity of the wetted film was calculated as the average between the emissivities of the studied liquid and the porous film.

The sample holder plastic plate with the 0.7 cm radius gap in the center was equipped with two copper electrical connections at the opposite edges of the gap on the bottom of the sheet. The BP was fixed to the bottom of the plastic section with magnetic clips. The copper electrodes were contacted to the source meter by 0.3 mm diameter copper wires. The rigidity of these wires did not affect the balance because of the large inertia of the whole assembly mounted on the balance plate. This was confirmed by independent experiments before the evaporation profile (electrical resistance variation as a function of time) measurements. The computer recorded the electrical resistance of the buckypaper as measured by a Keithley 2612A Source Meter.

Before the measurements, the BP film was mounted in the assembly and heating at initial temperature was applied until the electrical resistance and the sample weight both stabilized. Then all three recordings (resistivity, IR imaging and sample weight) were started a few seconds before dropping. The evaporation was studied by dropping a single droplet of a selected solvent to the center of the BP film and simultaneously recording the IR video, the mass and electrical resistance until they returned to their original values.

The schematics of the equipment is presented in Fig. 1. The ambient air temperature and the relative humidity of the ambient atmosphere were kept constant (at 25 °C and 55 RH%, respectively) [3-5].

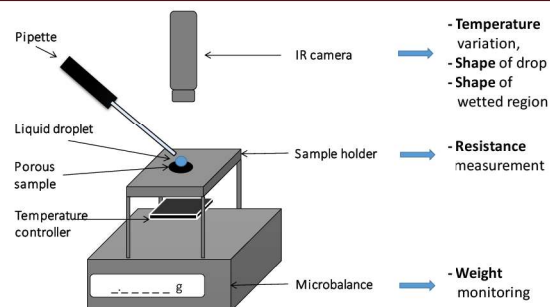


Figure 1. Evaporation monitoring equipment schematic.

Results and discussion

In general at the moment we drop the liquid on the buckypaper film (t_0), the liquid starts to diffuse immediately into the pores of the BP, but a part of it remains spread on the surface of the film. The evaporation of this liquid from the surface takes place together with the diffusion. Once all liquid evaporates from the surface, namely the primary surface evaporation is complete (t_s), liquid is left only in the pores. The solvent gradually evaporates from the pores as well because of the continuous heating. The complete evaporation of the solvent (t_t) was confirmed by the fact that the electrical resistance and mass of the buckypaper returned to the baseline.

One typical mass variation is illustrated in Fig. 2. where t_0 marks the time when the drop was instilled. The mass of the BP increased as soon as the solvent was dropped to the film and this is followed by a quasi-linear weight decrease. Once the primary surface evaporation is complete (t_s), the mass of the buckypaper decreases as linear (within experimental error) functions of time due to the continuous evaporation of the solvent. The total evaporation time (t_t) was at the moment when the mass of the BP returned to the baseline. At the linear weight decreasing ranges, the rate of evaporation (dm/dt) is constant. The change of dm/dt value suggests the change of the dominant evaporation process, e.g., evaporation of the droplet sitting on the surface of the BP, evaporation of the condensed water from the porous system or the evaporation of the adsorbed water from the microscopical surface of the porous system (see the linear ranges in Fig.2.). From this type of measurement, the typical experimentally determined data are the shape of the curve: m_{max} , area, FWHM; the t_s and t_t , the evaporation rate dm/dt and its change. These data are characteristic for the measured system and can be used to identify them [3-5].

The electrical resistance of the BP increased as soon as the solvent was dropped to the film. One typical resistance variation is illustrated in Fig. 2 where t_0 marks the time when the drop was instilled and t_s marks the time needed to surface evaporation. In case of typical organic solvents (e.g., 1-propanol, acetone, ethanol, etc.) the electrical resistance increases continuously between t_0 and t_s , because in this interval the solvent fills the pores of the BP film and the resistance of its solvent occupied section is higher than the liquid-free one. Once the primary surface evaporation is complete, the electrical resistance of the BP decreases as linear (within experimental error) functions of time due to the continuous evaporation of the organic solvent. Evaporation takes place both within the BP pores (resulting in vapor diffusing to the atmosphere) and from the surface where capillary forces continue to deliver liquid from the inside of the BP (secondary surface evaporation). Summarizing, when a droplet of solvent contacts a heated porous film, the electrical resistance of the film exhibits a very characteristic change as a function of time, which can be named as evaporation profile.

The shape of this curve is slightly different for every solvent and the fine details of the curve's shape can be described by the R_{max} , area, FWHM, t_s and t_t , etc. These data are characteristic for the measured system, too. For example, the shape of the evaporation profile depends strongly on the solvent in case of fixed solid, temperature and liquid volume (see Fig. 3.) or it depends strongly on the porous solid in case of fixed solvent, temperature and liquid volume (see Fig. 4.) [3-5].

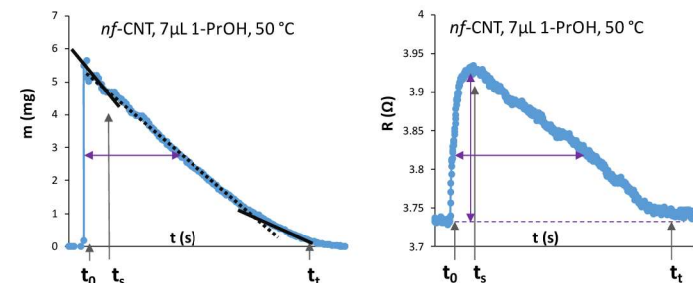
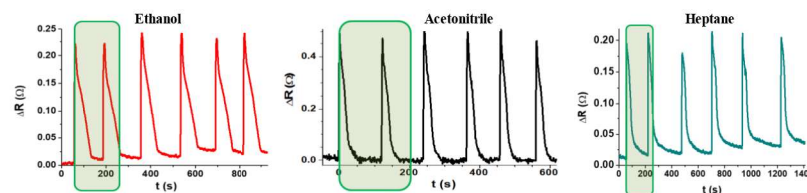
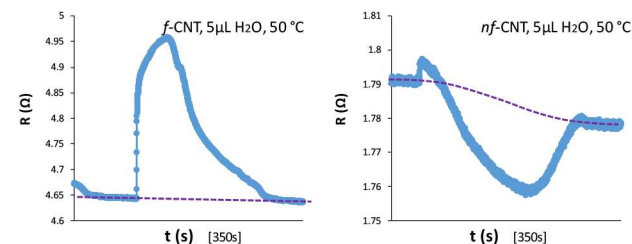


Figure 2. Weight and electrical resistance variation of the buckypaper as functions of time.

Figure 3. Evaporation profiles: solvent dependence. Evaporation of different organic solvents from *nf*-CNT buckypapers (5 μ L, 50 °C).Figure 4. Evaporation profiles: solid dependence. Evaporation of distilled water from *nf*-CNT and *f*-CNT buckypapers (5 μ L, 50 °C).

Infrared imaging is suitable to monitor the evaporation of the solvent from the porous film in our case from a vertical perspective. To improve the infrared contrast, solvents were kept at room temperature before the experiments. Therefore, there was a temperature difference between the initial 5 μ L drops and the porous film kept at 50 °C. The temperature of the liquid and the solid is changed continuously during the experiment because of the initial difference,

the heating of the solid layer, the endotherm evaporation process, etc. The videos were evaluated at selected representative moments, such a typical series of images is shown in Fig. 5. [3-5]. The temperature change profile is characteristic for each measured solvent. It is possible to determine the spot area and average temperature of the drop (S_d , T_d) and of the wetted region (S_w , T_w) as a function of time. Usually, we use relative timescale ($t_{rel} = t/t_s$) for comparable representation. Some data extracted from infrared videos are characteristic for the evaporation of a selected liquid/solid system: surface evaporation time (t_s), total evaporation time (t_t), initial area of the drops ($S_{d(t_0)}$), area of the wetted region at the end of the surface evaporation ($S_{w(t_s)}$). The change of S_d as a function of time can give information about the mechanism of the evaporation (*e.g.*, constant contact radius mode - CCR) and the relationship between S_d and S_w can describe the wetting degree of the porous system.



Figure 5. Images exported pro rata from the IR video correspond to t_0 , t_s , t_t and several representative intermediate times (*nf*-CNT, 5 μ L H_2O , 50°C).

Conclusion

The simultaneous weight monitoring, electric resistance measurement and infrared imaging of the evaporation of liquids from porous films can provide information about the mechanism of wetting and vaporization which is a significant area of the basic researches. Furthermore, it can be proved by using appropriate statistical methods (*e.g.*, matrix of Pearson correlation coefficients, hierarchical cluster analysis, functional analysis, etc.), that the experimentally determined characteristic values are specific for the physical properties of the solvents, and they are also dependent on the quality of the solid materials, therefore, they can be used for qualitative chemical analysis via the estimation of physical properties. The results allow us to presume the possibility of this experimental setup and theoretical approach for a potential future application in the field of analytics.

Acknowledgements

Financial support from the Hungarian National Research, Development and Innovation Office through the GINOP-2.3.2-15-2016-00013 “Intelligent materials based on functional surfaces—from syntheses to applications” project, the Ministry of Human Capacities, Hungary, grant 20391-3/2018/FEKUSTRAT and the János Bolyai Research Fellowship of the Hungarian Academy of Sciences is acknowledged.

References

- [1] D. Bonn, J. Eggers, J. Indekeu, J. Meunier, E. Rolley, *Mod. Phys.* 81(2) (2009) 739–804.
- [2] H.Y. Erbil, *Adv. Colloid Interface Sci.* 170(1-2) (2012) 67–86.
- [3] G. Schuszter, E.S. Bogya, D. Horváth, Á. Tóth, H. Haspel, Á. Kukovecz, *Mic. Mes. Mat.* 209 (2015) 105–112.
- [4] E.S. Bogya, B. Szilagyi, Á. Kukovecz, *Carbon* 100 (2016) 27–35.
- [5] Á. Kukovecz, *Egydimenziós nanoszerkezetek és hálózataik létrehozása, módosítása és néhány felhasználási lehetősége*, MTA értekezés, Szeged, 2018